

# Locking a microsphere whispering-gallery mode to a laser

J. P. Rezac and A. T. Rosenberger

Department of Physics and Center for Laser and Photonics Research,  
Oklahoma State University, Stillwater, Oklahoma 74078-3072  
atr@okstate.edu

**Abstract:** We have locked a whispering-gallery resonance of a fused-silica microsphere to a frequency-scanning laser. The resonance frequency is modulated by axial compression of the microsphere, and phase-sensitive detection of the fiber-coupled optical throughput is used for locking. Using a laser wavelength of either 1570 nm or 830 nm, we demonstrate a locked tracking range exceeding 30 GHz for a microsphere of 120 GHz free spectral range. This performance has been enabled by an improved compression tuner design that allows coarse tuning over 1 THz and piezoelectric tuning over 80 GHz. Compression modulation rates of up to 13 kHz have also been achieved with this tuner.

©2001 Optical Society of America

**OCIS codes:** (230.5750) Resonators; (140.4780) Optical resonators; (060.2340) Fiber optics components

---

## References and links

1. V. B. Braginsky, M. L. Gorodetsky, and V. S. Ilchenko, "Quality factor and nonlinear properties of optical whispering-gallery modes," *Phys. Lett. A* **137**, 393-397 (1989).
2. D. W. Vernooy, V. S. Ilchenko, H. Mabuchi, E. W. Streed, and H. J. Kimble, "High- $Q$  measurements of fused-silica microspheres in the near infrared," *Opt. Lett.* **23**, 247-249 (1998).
3. D. W. Vernooy, A. Furusawa, N. Ph. Georgiades, V. S. Ilchenko, and H. J. Kimble, "Cavity QED with high- $Q$  whispering gallery modes," *Phys. Rev. A* **57**, R2293-R2296 (1998).
4. V. V. Vassiliev, V. L. Velichansky, V. S. Ilchenko, M. L. Gorodetsky, L. Hollberg, and A. V. Yarovitsky, "Narrow-line-width diode laser with a high- $Q$  microsphere resonator," *Opt. Commun.* **158**, 305-312 (1998).
5. W. von Klitzing, E. Jahier, R. Long, F. Lissillour, V. Lefèvre-Seguin, J. Hare, J.-M. Raimond, and S. Haroche, "Very low threshold green lasing in microspheres by up-conversion of IR photons," *J. Opt. B: Quantum Semiclass. Opt.* **2**, 204-206 (2000).
6. M. Cai, O. Painter, K. J. Vahala, and P. C. Sercel, "Fiber-coupled microsphere laser," *Opt. Lett.* **25**, 1430-1432 (2000).
7. D. Braunstein, A. M. Khazanov, G. A. Koganov, and R. Shuker, "Lowering of threshold conditions for nonlinear effects in a microsphere," *Phys. Rev. A* **53**, 3565-3572 (1996).
8. A. T. Rosenberger, "Nonlinear Optical Effects in the Whispering-Gallery Modes of Microspheres," in *Operational Characteristics and Crystal Growth of Nonlinear Optical Materials*, R. B. Lal and D. O. Frazier, eds., *Proc. SPIE* **3793**, 179-186 (1999).
9. A. T. Rosenberger and J. P. Rezac, "Evanescent-wave sensor using microsphere whispering-gallery modes," in *Laser Resonators III*, A. V. Kudryashov and A. H. Paxton, eds., *Proc. SPIE* **3930**, 186-192 (2000).
10. I. H. Malitson, "Interspecimen Comparison of the Refractive Index of Fused Silica," *J. Opt. Soc. Am.* **55**, 1205-1209 (1965).
11. V. S. Ilchenko, P. S. Volikov, V. L. Velichansky, F. Treussart, V. Lefèvre-Seguin, J.-M. Raimond, and S. Haroche, "Strain-tunable high- $Q$  optical microsphere resonator," *Opt. Commun.* **145**, 86-90 (1998).
12. W. von Klitzing, R. Long, V. S. Ilchenko, J. Hare, and V. Lefèvre-Seguin, "Frequency tuning of the whispering-gallery modes of silica microspheres for cavity quantum electrodynamics and spectroscopy," *Opt. Lett.* **26**, 166-168 (2001).
13. W. von Klitzing, R. Long, V. S. Ilchenko, J. Hare, and V. Lefèvre-Seguin, "Tunable whispering gallery modes for spectroscopy and CQED experiments," <http://arXiv.org/abs/quant-ph/0011102>.
14. J. C. Knight, G. Cheung, F. Jacques, and T. A. Birks, "Phase-matched excitation of whispering-gallery mode resonances by a fiber taper," *Opt. Lett.* **22**, 1129-1131 (1997).
15. M. Cai, O. Painter, and K. J. Vahala, "Observation of Critical Coupling in a Fiber Taper to a Silica-

In a dielectric microsphere, an optical whispering-gallery mode (WGM) consists of light propagating around the equator, spatially confined to a narrow beam near the sphere's surface by total internal reflection. The extremely low WGM losses of fused-silica microspheres allow them to be used as high- $Q$  microresonators [1,2]. Such microresonators have the potential to be used in many areas, including cavity quantum electrodynamics [3], laser stabilization [4], microlasers [5,6], nonlinear optics [7,8], and evanescent-wave sensing [9]. The utility of WGM microresonators can be greatly enhanced by making their resonant frequencies tunable. One way to tune WGM resonances is by changing the temperature of the sphere [3]. This gives at most a  $2.5/\lambda$  GHz/K shift ( $\lambda$  in  $\mu\text{m}$ ), primarily due to change in the refractive index [10], but the effect is slow and its practical range is limited. A better tuning method makes use of axial compression [11] or stretching [12,13] of the microsphere. The corresponding change in optical path length for WGMs allows fast tuning over much of a free spectral range (FSR).

In this article we report a new application for a compression tuner and the advances in compression tuning that make it possible. The advances include extending the tuning range (in units of the FSR) and enhancing the response speed; these enable locking to a laser, keeping a single WGM on resonance as the laser frequency is scanned. For our experiments, a microsphere was fabricated by torch-melting the end of an optical fiber; the microsphere used in this work had a diameter of 550  $\mu\text{m}$ . A tapered fiber in contact with the sphere was used for coupling to the WGMs [14,15]. Light from a tunable laser, either an extended-cavity diode used at 1570 nm or a cw Ti:sapphire used at 830 nm, was launched into a single-mode fiber (SMF-28) that was angle-polished at the injection face ( $8^\circ$  from normal) to prevent back reflection into the laser. In the fiber-microsphere coupling region, the fiber was tapered by heating and stretching a short section to a diameter of 20  $\mu\text{m}$  or less, followed by hydrofluoric-acid etching to a 5-10  $\mu\text{m}$  diameter. A fiber polarization controller allowed excitation of either tangentially polarized (TE) or radially polarized (TM) WGMs. The fiber throughput was detected as either the laser or microsphere was tuned, with sharp dips in transmitted power indicating the excitation of WGMs. The width of a dip gave a loaded-sphere quality factor  $Q$  of (typically)  $2 \times 10^6$ . Although better than 90% extinction could be achieved using optimal taper size and alignment, in these experiments the typical extinction was about 20%.

Besides the polarization, three integers are needed to specify a WGM. The mode number  $\ell$  is, approximately, the number of wavelengths in the sphere's circumference. The mode order  $q$  is the number of radial intensity maxima, and  $\ell - |m| + 1$  (where  $|m| \leq \ell$ ) gives the number of maxima in "latitude". The "fundamental" WGM has  $q = 1$  and  $|m| = \ell$  and thus a single transverse maximum. The WGM resonant frequencies are approximately [4]

$$\mathbf{v}_{q\ell m}^i = \delta \left[ \ell + \frac{1}{2} + A_q \left( \frac{\ell + 1/2}{2} \right)^{1/3} - \Delta^i + (\ell - |m|) \frac{a_e - a_a}{a} \right] \quad (1)$$

In Eq. (1),  $i$  denotes TE or TM,  $\delta = c / 2\pi a_e n$  is the microsphere's nominal free spectral range,  $n$  is the index of refraction of the sphere,  $a$  is the sphere radius ( $a_e$ , equatorial;  $a_a$ , axial), the  $\Delta^i$  are polarization-dependent shifts, and  $A_q$  is the  $q^{\text{th}}$  zero of the Airy function:  $\text{Ai}(-A_q) = 0$ . In forming a microsphere, a small amount of eccentricity results, so that  $a_e$  and  $a_a$  typically differ by about 1% [4,11]. Axial compression of the microsphere results in tuning of the WGM frequencies, given in terms of the fractional change in axial radius as

$$\frac{\Delta\nu}{\nu} = \frac{\Delta a_e}{a} \mu \left[ 1 + b^i - \left( \frac{1+\mu}{\mu} \right) \frac{\ell - |m|}{\ell} \right]. \quad (2)$$

The first and second terms in Eq. (2) come from the changes in  $\delta$  due to changes in  $a_e$  and  $n$ , respectively. The third term results from the change in eccentricity, and tuning due to the change in  $\Delta^i$  is negligible. Because our tuner's contact-surface configuration is not too different from that of Ref. 11, we use their strain calculation results to estimate the relative contributions of the three terms. Specifically, we take the effective Poisson ratio  $\mu$  to be  $\mu = |\Delta a_e / \Delta a_a| = 0.11$  (rather than the handbook value of 0.17) and the photoelastic contribution to be  $b^{TE} = -0.14$  or  $b^{TM} = 0.07$ . Since  $\ell \approx 1500$  for our sphere at 1570 nm, the third term contributes -0.16 for  $\ell - |m| = 24$ , and so the geometrical path length change given by the first term in Eq. (2) dominates the tuning. (The value of  $\ell - |m| = 24$  used above is an estimate for the maximum observed here, as very long frequency scans showed families of 20-25 modes with  $\sim 1$  GHz spacing, each with a bandhead that is probably the  $|m| = \ell$  mode.)

Our compression tuner is shown in Fig. 1. To improve the tuner's response speed, its moving mass was minimized by using aluminum except for the compression pads at the ends of the two cantilever arms. Flexing of the lower arm preloads the piezoelectric actuator (PZT). The flexibility of the upper arm allows the design to accommodate a large range of microsphere sizes. During fabrication, a short axial stem is left attached to the microsphere, which is then mounted in the tuner by inserting the stem into a short length of hypodermic tubing having an outer diameter of 300  $\mu\text{m}$  and an inner diameter of 50  $\mu\text{m}$ . The lower surface contacting the sphere (indented tubing end) thus has a diameter approximately equal to half that of the sphere, as in Ref. 11. No permanent indentation was noticed in the upper compression pad, so its contact diameter was presumably somewhat smaller than that of the lower surface. The qualitative conclusions of the previous paragraph, based on the strain analysis of Ref. 11, are therefore reasonable. Since tubing is used to hold the sphere, there is a lower limit on microsphere diameter for this tuner. For spheres larger than 300  $\mu\text{m}$ , using tubing above as well as below the sphere would facilitate prism coupling.

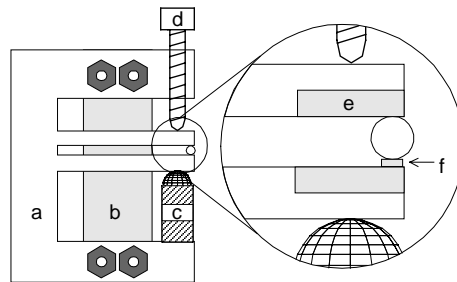


Fig. 1. Compression tuner. (a) Main body is 44×38×6-mm aluminum. (b) Stainless steel brace minimizes flexing of main body. (c) Piezoelectric actuator. (d) Manual tuning screw. (e) Hardened steel compression pad. (f) Stainless steel hypodermic tubing, inserted into hole in lower steel pad.

The absolute tuning ranges that we report below are smaller than in previous demonstrations [11-13], but only because we used larger microspheres. Our objective was to improve the effectiveness of the tuner. As Eq. (2) shows, the tuning of a WGM frequency is proportional to the axial compression and to the WGM frequency, and inversely proportional to the microsphere radius. Since the FSR is also inversely proportional to microsphere radius, the ratio of tuning to FSR is a figure of merit for tuning effectiveness that is

independent of microsphere size. The ratio is still essentially proportional to frequency, so, for purposes of comparison to previously achieved tuning/FSR ratios, we report tuning results at 830 nm as well as at our primary wavelength of 1570 nm.

Our microsphere had a nominal FSR of 120 GHz. Adjustment of the manual tuning screw allows coarse tuning over several free spectral ranges, permitting a choice of which set of modes to make accessible to PZT tuning. The manual tuning range was approximately 500 GHz at 1570 nm and 1 THz at 830 nm. Applying PZT voltages of 0-150 V gave a fine-tuning range of 36 GHz at 1570 nm and 80 GHz at 830 nm. The latter value, expressed as two-thirds of a FSR, is better than previously reported [11-13], indicating increased tuning effectiveness. The observed PZT-tuning ranges imply an axial diameter compression of approximately 1  $\mu\text{m}$ , less than the 7  $\mu\text{m}$  expected for a 150-V bias, but a larger fraction than in previous work [11], probably due to our use of harder contacting materials. In addition, increasing the force applied by the manual tuning screw increases the efficiency of PZT microsphere compression, presumably because much of the deformation of the contacting surfaces is done before voltage is applied to the PZT. This efficiency increase was recently demonstrated using a 300- $\mu\text{m}$  diameter microsphere, where tuning of nearly two-thirds of a FSR was achieved at 1570 nm. If measured at 830 nm, this would have been about 1.2 FSR, or 265 GHz. The tuning ranges were measured by scanning the laser and noting the mode displacement with PZT bias, as shown in Fig. 2(a)-(d). The frequency scale was calibrated using a commercial confocal spectrum analyzer with a 2-GHz FSR. The tuning speed was measured by applying a 5-V peak-to-peak sinusoidal modulation to the PZT. The maximum was at least 16 GHz/ms; we could get significant tuning at a modulation rate of up to 13 kHz, thirty times faster than before [11], due to the lighter tuner design.

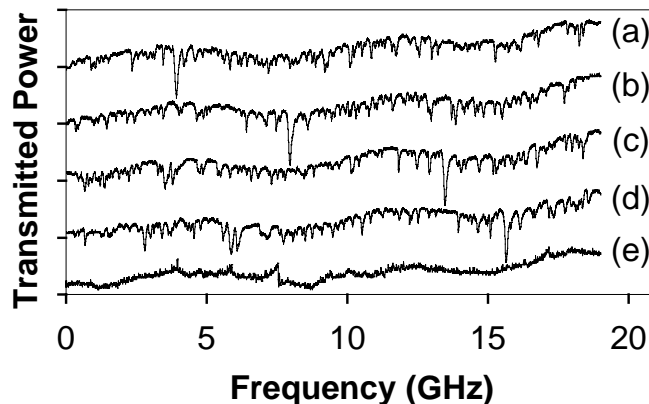


Fig. 2. Unlocked and locked frequency scans at 1570 nm. (a)-(d) Unlocked: WGM mode spectrum observed as the laser is scanned over a 19 GHz range; an increasing frequency shift is seen for PZT bias voltages of 68 V, 88 V, 118 V, and 130 V, respectively. The baseline for trace (a) is at the frequency axis, and successive traces have been displaced vertically. (e) Locked: frequency scan where the WGM with the deepest dip in (a)-(d) is locked to the laser. The baseline is the same as for trace (d). No mode hops are observed.

For locking a WGM to the laser, we used a commercial lock-in stabilizer designed for the stabilization of CO<sub>2</sub> lasers. Its 518 Hz locking modulation signal and dc bias were combined in a capacitive voltage divider for application to the PZT; the applied locking modulation was a 30-60 mV peak-to-peak dither and the applied bias was 0-150 V. We chose to lock under conditions that would provide a stringent test of the stability of the technique and so provided no isolation from building vibration or air currents. Furthermore, the diameter and alignment of the coupling fiber taper were chosen so that many modes were excited, as seen in Fig. 2,

where the 1570-nm laser was scanned over 19 GHz. The four laser frequency scans in traces (a)-(d) of Fig. 2 are over the same range, with different constant bias voltages (and no locking dither) applied to the PZT. All modes have the same polarization here, but there is some variability in their relative positions from (a) through (d) because of the slightly different tuning rates for modes of different  $m$ . The deepest dip, indicating about 20% extinction and  $Q \approx 2 \times 10^6$ , is the one to which we locked. A scan of the same range, with that mode now locked to the laser, is shown in Fig. 2(e). Note that the slow power variation (from frequency dependence of the fiber transmission) is the same in (a)-(e). From (e), it is evident that the locking never switches to a different mode, because doing so would result in an obvious displacement of the trace. The larger fluctuations on this trace may indicate the temporary overlap of a differentially-tuning mode with the locked one; the noise level is consistent with the approximately 150 mV peak-to-peak high-frequency noise on the PZT bias. As a result of this noise, which is made up of frequency components in the several-kHz range, too fast to be compensated by the 518 Hz locking dither, the effective lock point fluctuates with an amplitude of about one-fifth of the 90-MHz WGM linewidth. Fig. 3 shows a back-and-forth scan of 8 GHz with more uniform fiber transmission, illustrating the constancy of locked-mode power throughput that is achievable with our locking method.

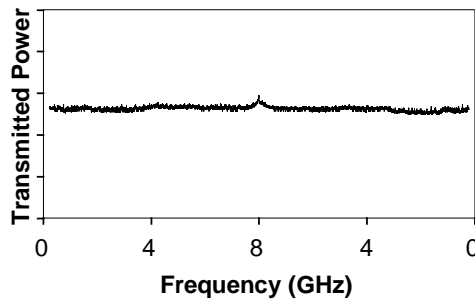


Fig. 3. Another locked frequency scan at 1570 nm. The laser scans 8 GHz and returns. The vertical scale is the same as in Fig. 2. The baseline is at the frequency axis and again the locked transmission is about 80% of its off-resonance value. No mode hops are observed.

Another verification of the robustness of WGM locking and tracking is shown in Fig. 4. There, the PZT bias that keeps a WGM locked to the 1570-nm laser (New Focus, model 6328) is plotted as the tuning control signal applied to the laser's frequency-modulation input is ramped up and down. This is again the 19 GHz tracking range shown in Fig. 2. Ideally, the WGM frequency would vary linearly with the tuner bias, and the laser frequency would vary linearly with the control voltage. However, the variation of laser frequency with control voltage shows hysteresis. Assuming the tuner PZT to be linear, the red curve in Fig. 4 is the bias predicted from the laser frequency tuning as observed with an optical spectrum analyzer. Comparison of the two curves in Fig. 4 shows that most of the hysteresis seen in the bias is actually hysteresis in the laser tuning, with only a small contribution from the nonlinearity of the compression tuner's PZT. A mode jump would appear as a displacement of the bias curve by an amount on the order of ten times the noise level, and none are seen. The locking and tracking range shown in Figs. 2 and 4 is 19 GHz, but we were able to extend this to 30 GHz, the maximum scan range of the 1570-nm laser. Locking to the 830-nm laser worked equally well, and again the maximum tracking range was limited only by the laser's frequency scan range of 40 GHz. At 830 nm the WGMs had, typically,  $Q \approx 5 \times 10^6$ . Even under the environmentally noisy conditions that we used here, a WGM would remain locked to either laser for hours, with the laser scanning at rates of up to 2 GHz/s.

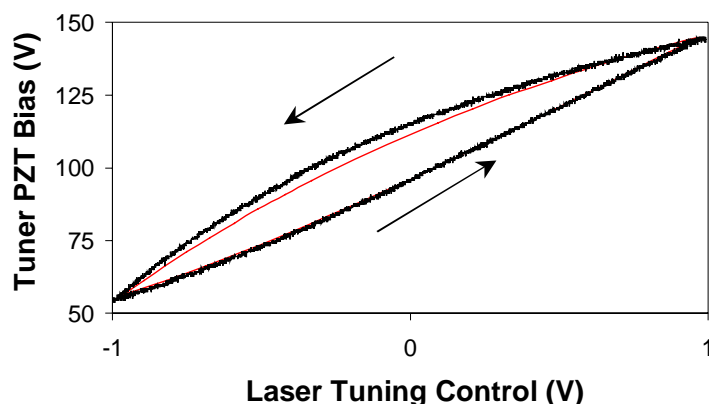


Fig. 4. Locked tuner PZT bias as it follows a 19-GHz frequency scan (and return) of the 1570-nm laser. Heavier (black) curve: PZT bias; no mode hops are observed. Lighter (red) curve: bias predicted from observed laser tuning hysteresis, assuming linear tuner PZT response.

Our results for WGM frequency tuning and locking are summarized in Table 1. Our compression tuner allows for tuning over a greater fraction of a free spectral range, and with faster response, than previously demonstrated [11-13]. The ability to lock a high- $Q$  WGM to a frequency-scanning laser will be useful for a number of potential applications of microsphere resonators. For example, the tracking range demonstrated is more than sufficient for doing wavelength-modulation spectroscopy in WGM evanescent-wave trace gas sensors. The maximum laser scan rate at which a WGM will remain locked, 2 GHz/s, is determined by the locking dither frequency and the  $Q$  value of the WGM. Locked scanning must be slow enough that the frequency change during one dither cycle is small compared to the WGM linewidth. To increase the maximum scan rate, it would be desirable to frequency-modulate the laser output to provide a faster locking dither. Then the locked scan rate would be limited only by the maximum compression tuning speed, which we found to be at least 16 GHz/ms. Thus locked modes of  $Q = 2 \times 10^6$  could follow a scan nearly four orders of magnitude faster, or locked modes of  $Q \cong 10^{10}$  could be scanned at the present rate.

Table 1. Tuning ranges for a 550- $\mu\text{m}$  diameter microsphere at two wavelengths

Range	1570 nm	830 nm
FSR	120 GHz (1.0 nm)	120 GHz (0.27 nm)
Manual	500 GHz (4.2 nm)	1000 GHz (2.2 nm)
PZT	36 GHz (0.30 nm)	80 GHz (0.18 nm)
Locked*	30 GHz (0.24 nm)	40 GHz (0.09 nm)

\*Limited by the lasers' continuous tuning ranges

### Acknowledgments

This work was supported by the Center for Sensors and Sensor Technologies, the Environmental Institute, the Oklahoma Center for the Advancement of Science and Technology, and by the National Science Foundation through an SBIR with Nomadics, Inc. We thank Reza Mofid, Sarah Bates, and Mike Lucas for assistance.